RESEARCH ARTICLE

Nell-1-ΔE, a novel transcript of Nell-1, inhibits cell migration by interacting with enolase-1

Huaxiang Zhao[1] | Xueyan Qin[1] | Qian Zhang[2] | Xinli Zhang[3] |
Jiuxiang Lin[1] | Kang Ting[3] | Feng Chen[2]

[1] Department of Orthodontics, Peking University School and Hospital of Stomatology, Beijing, P. R. China

[2] Central Laboratory, Peking University School and Hospital of Stomatology, Beijing, P. R. China

[3] Dental and Craniofacial Research Institute, University of California, Los Angeles, California

Correspondence
Jiuxiang Lin, Department of Orthodontics, Peking University School and Hospital of Stomatology, 100081, Beijing, P. R. China.
Email: jxlin@pku.edu.cn
Kang Ting, Dental and Craniofacial Research Institute, University of California, Los Angeles 90095, CA.
Email: kting@ucla.edu
Feng Chen, 22 Zhongguancun South Avenue, Haidian District, 100081, Beijing, P. R. China.
Email: moleculecf@gmail.com

Funding information
National Natural Science Foundation of China, Grant number: 81200762; NIH/NIDCR, Grant numbers: R21, DE0177711, RO1, DE01607; UC Discovery, Grant number: 07-10677

Abstract

NELL-1 is a secreted protein that was originally found to be upregulated in pathologically fusing and fused sutures in non-syndromic unilateral coronal synostosis patients. Apart from the ability of NELL-1 to promote osteogenesis in long and craniofacial bones, NELL-1 reportedly inhibits the formation of several benign and malignant tumors. We previously identified a novel transcript of *Nell-1* that lacked a calcium-binding epidermal growth factor (EGF)-like domain compared with full-length *Nell-1*; this new transcript was named *Nell-1-ΔE*. Three obvious structural differences between these two isoforms were revealed by homology modeling. Furthermore, the recombinant Nell-1-ΔE protein, but not the full-length Nell-1 protein, inhibited cell migration in vitro. However, full-length Nell-1 and Nell-1-ΔE proteins were present in similar subcellular locations and displayed similar expression patterns in both the intracellular and extracellular spaces. The results from the co-immunoprecipitation and liquid chromatography/tandem mass spectrometry analyses using two cell lines demonstrated that Nell-1-ΔE but not full-length Nell-1 interacted with enolase-1 in the extracellular spaces of both cell lines. The results of wound healing assays using ENO-1-overexpressing cells treated with full-length Nell-1/Nell-1-ΔE suggested that Nell-1-ΔE inhibited cell migration by interacting with ENO-1. Our study indicated that the novel transcript *Nell-1-ΔE*, but not full-length *Nell-1*, might be a candidate tumor suppressor factor for basic research and clinical practice.

KEYWORDS
alpha-enolase, cell migration assays, isoforms, nel-like protein 1, protein-protein interaction, proteomics

1 | INTRODUCTION

The Nel-like molecule, type 1 (NELL-1) protein is a secretory glycoprotein that belongs to the NELL family,[1] together with NELL-2.[2,3] *NELL-1* is overexpressed in the pathologically fusing and fused sutures of non-syndromic unilateral coronal synostosis (CS) patients.[4] Major skeletal system abnormalities were observed in *Nell-1*-deficient mice,[5] whereas CS-like phenotypes were found in mice that overexpressed *Nell-1*.[6] These findings implicate NELL-1 as an important protein in embryonic development.

In our previous study, we performed polymerase chain reaction (PCR) on two segments of rat cDNA that were extracted from a cDNA library to obtain a *Nell-1* clone. Upon

gel electrophoresis of Segment 2, a second band with a lower molecular weight was observed in addition to the band of the expected molecular weight. Sequencing of the lower molecular weight band revealed a new transcript of *Nell-1*, which lacked sequences that encoded a calcium-binding epidermal growth factor (EGF)-like domain compared with full-length *Nell-1*. This novel transcript was designated *Nell-1-ΔE* (ΔE denotes the deleted calcium-binding EGF-like domain).[4] A recent study reported that a short isoform of NELL-1 might have one function that is distinct from that of full-length NELL-1.[7] Considering the important role of the Ca^{2+}-binding EGF-like domain in protein-protein interactions,[8] we speculated that Nell-1-ΔE might have particular features that distinguish it from full-length Nell-1. Meanwhile, Nell-1-ΔE is widely conserved in humans, mice, rhesus macaques, and naked mole rats (data from UniProt; http://www.uniprot.org/). The high conservation of Nell-1-ΔE enlightens us that this isoform might have important functions.[3,4]

In this study, by homology modeling, we compared the difference in the predicted structure between full-length Nell-1 and Nell-1-ΔE and observed obvious differences. Wound healing assays and the iCELLigence Real-Time Cell Analysis system, which were used to compare the effects of these two isoforms on cell migration, demonstrated that Nell-1-ΔE, but not full-length Nell-1, inhibited cell migration. Furthermore, when we compared the subcellular localization and expression patterns of these two proteins, no obvious differences were observed. To investigate the interaction between these two secretory proteins in the extracellular space, the medium was collected from cells that overexpressed one of these two isoforms. Co-immunoprecipitation (co-IP) and liquid chromatography/tandem mass spectrometry (LC-MS/MS) analyses of the media revealed that Nell-1-ΔE but not full-length Nell-1 interacted with enolase-1 (ENO-1) in the extracellular space.

2 | MATERIALS AND METHODS

2.1 | Cell culture

A murine immortalized mineralized cell line for cementoblasts, OCCM-30,[9] was used as in our previous study.[10] Human embryonic kidney epithelial cells, HEK-293FT and HEK-293T, were gifts from Dr. Chen.[11] The LoVo human colorectal adenocarcinoma cell line was a gift from Dr. Wang (Peking University). All cells were maintained as monolayer cultures in Dulbecco's modified Eagle's medium (DMEM; Life Co., Grand Island, NY) and cultured in an incubator (37°C, 5% CO_2).

2.2 | Plasmid construction

The mouse full-length *Nell-1* coding sequence[12] was cloned into the pEGFP-N2 vector (Clontech, Shiga, Japan),

p3 × FLAG-CMV™-14 Expression Vector (Sigma, St. Louis, MO), and a pmCHERRY-N1 vector (Clontech) and designated Nell-1-GFP, Nell-1-FLAG, and Nell-1-CHERRY, respectively. The mouse *Nell-1-ΔE* coding sequence (Ensembl transcript ID: ENSMUST00000107603.1) was generated from the mouse full-length *Nell-1* plasmid by inverse-PCR and cloned into a pEGFP-N2 vector and the p3 × FLAG-CMV™-14 Expression Vector; these two constructs were designated Nell-1-ΔE-GFP and Nell-1-ΔE-FLAG.

2.3 | RNA isolation and PCR

Total RNA was extracted from the cranial meninges, cerebral hemispheres, medulla oblongatas, and whole heads of Kunming mice on embryogenic day 14 (E14), E16, and E19 using the TRIzol® Reagent (Invitrogen, Carlsbad, CA). To determine the expression ratio of *Nell-1-ΔE* to full-length *Nell-1*, forward (5′-ggtaaaaatcacagaagcttgccc-3′) and reverse (5′-gttattctcaagacacaccagatcc-3′) primers spanning the second calcium-binding EGF-like domain were used to amplify cDNA by Taq PCR (Cwbiotech, Beijing, China). All animals were cared for according to the institutional guidelines of Peking University (Animal Ethics Number: LA2013-92).

2.4 | Wound healing assay and iCELLigence real-Time cell analysis system

LoVo cells were seeded in 6-well plates at a density of 1×10^6 cells per well. When the cells became confluent, a wound was generated using a p200 pipette tip to scratch the monolayer. Each scratch was approximately the same width in each well. Wounds were photographed at 0 and 24 h.

The iCELLigence Real-Time Cell analysis system (ACEA Bioscience Inc., San Diego, CA) is a non-invasive and label-free approach for measuring the cell growth rate and cell migration, based on changes of electrical impedance on the surface of well.[13,14] LoVo cells were seeded at a density of 1×10^5 cells per well. Between 24 and 30 h after cell seeding, full-length Nell-1 and Nell-1-ΔE proteins were added to the cultures, and the cells were continuously monitored for $144 \sim 168$ h.

2.5 | Proliferation assay

LoVo cells were seeded in 96-well plates at a density of 1×10^4 cells per well and treated with full-length Nell-1 and Nell-1-ΔE proteins (50 ng/mL). At 0, 12, 24, and 36 h, we added CCK-8 reagent (Dojindo, Kumamoto, Japan) to the plates and incubated at 37°C for 2 h. The absorbance at 450 nm was detected using a microplate reader.

2.6 | Transient transfection

For transient transfections, cells were seeded into dishes. After reaching >70% confluence at 12-24 h, OCCM-30, LoVo, and HEK-293FT cells were transfected using the Avalanche Transfection™ Reagent (EZ Biosystem, College Park, MD), Lipofectamine 3000® Reagent (Invitrogen), and FuGENE HD® Reagent (Promega, Madison, WI), respectively, in accordance with the manufacturer's instructions.

2.7 | Subcellular locations of full-length nell-1 and nell-1-ΔE proteins

Following co-transfection of Nell-1-CHERRY and Nell-1-ΔE-GFP into OCCM-30, cells were fixed using paraformaldehyde (4%) for 20 min on ice. Triton-X100 (0.5%) was added to the cells to increase permeability; DAPI staining (Solarbio, Beijing, China) was used to visualize cell nuclei. Images were captured by confocal microscopy (60 × magnification; Zeiss, Oberkochen, Germany).

2.8 | Co-immunoprecipitation

The medium was replaced with E8 serum-free medium (Life Co.) 42 h after transfection to prevent fetal bovine serum interference with the co-IP procedure. Six hours later, 4 mL medium was collected and centrifuged at $500 \times g$ for 5 min at 4°C. A protease inhibitor cocktail (Cwbiotech) was added to the supernatants, which were then incubated with 3 μL of rabbit anti-GFP antibody (a gift from Dr. Chen at Tsinghua University) overnight, followed by incubation with 40 μL of Protein A Magnetic Beads (Thermo Scientific, Waltham, MA) at room temperature for 1 h. Subsequently, each antigen-antibody-bead complex was washed three times at room temperature. Finally, co-immunoprecipitated complexes were resuspended in 70 μL of 1 × SDS-PAGE Loading Buffer (Cwbiotech) and then centrifuged at $12\,000 \times g$ for 5 min at 4 °C. Supernatants were collected for subsequent experiments.

2.9 | Western blotting

Thirty micrograms of the cell lysates, 20 μL medium or 20 μL of the co-IP products were separated by 8% SDS-PAGE under reducing conditions and transferred to PVDF membranes (Cwbiotech). Proteins were probed with a primary mouse anti-GFP antibody (Cell Signaling Technology, Danvers, MA) at a dilution of 1:1000 or with a mouse anti-FLAG antibody (Sigma) at a dilution of 1:5000. Membranes were then incubated with a fluorescent secondary antibody. Proteins were visualized using the Odyssey® LI-COR Imaging System (LI-COR Biotechnology, Lincoln, NE).

2.10 | Mass spectrometry and data analysis

Co-IP products (50 μL) were separated by 10% SDS-PAGE under reducing conditions. Gel lanes containing samples were cut into three pieces, dissolved in methanol, and loaded on an LTQ OrbitrapVelos instrument (Thermo Scientific). Protein IDs and original amounts were obtained from the LC-MS/MS mass spectra. Raw data from the LC-MS/MS were searched using UniProt database (http://www.uniprot.org/). A Venn diagram was used to analyze candidate proteins using the Bioinformatics & Evolutionary Genomics tool (http://bioinformatics.psb.ugent.be/webtools/Venn/).

2.11 | Homology modeling of full-length nell-1 and nell-1-ΔE protein structures

We used the three-dimensional structure of Notch ligand Delta-like 1 (PDB code 4xbm) and the internal ligand-bound, metastable state of a leukocyte integrin (PDB code 4neh) to construct a structural model of full-length Nell-1 and Nell-1-ΔE proteins using SWISS-MODEL (http://swissmodel.expasy.org/).[11]
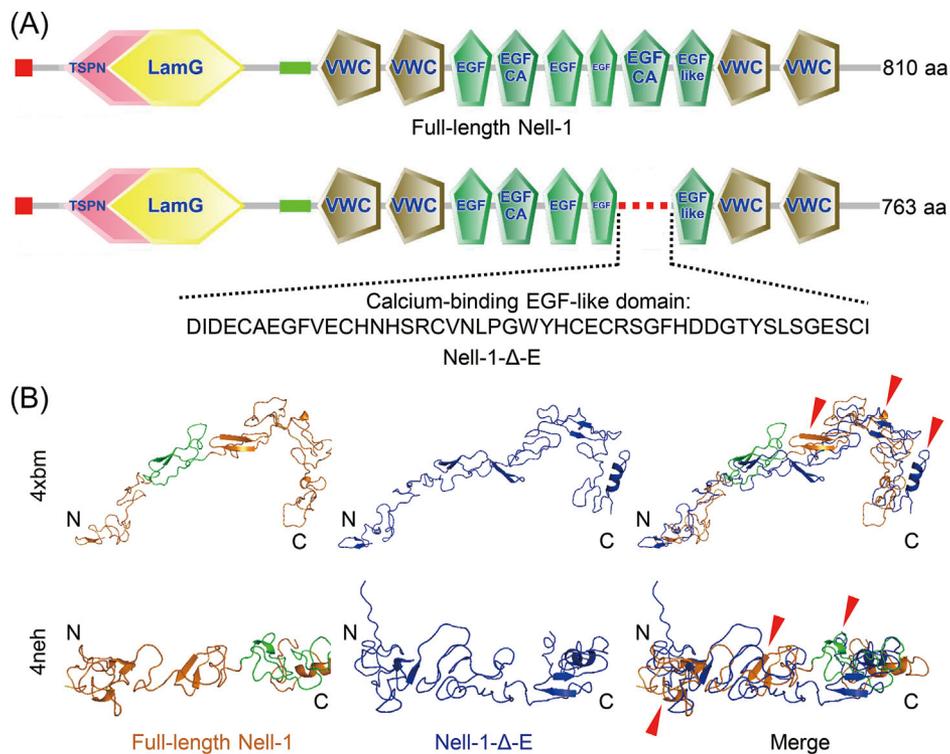
2.12 | Statistics

Values were presented as the mean ± standard deviation. Significant differences between two groups were calculated using Student's t-test. $P < 0.05$ was considered statistically significant.

3 | RESULTS

3.1 | Differences in structure between full-length nell-1 and nell-1-ΔE as predicted by homology modeling

In our previous study, we unexpectedly discovered a novel transcript of *Nell-1* when we cloned rat *Nell-1*.[4] Because the transcript lacked a sequence that encoded a calcium-binding EGF-like domain compared with full-length *Nell-1*, we named the variant *Nell-1-ΔE* (Figure 1A). First, we aimed to determine the differences in structure between full-length Nell-1 and Nell-1-ΔE due to the absent calcium-binding EGF-like domain in Nell-1-ΔE (Figure 1A). Homology modeling was performed based on the structure of Notch ligand Delta-like 1 (4xbm) (Figure 1B, upper panel) or the leukocyte integrin (4neh) (Figure 1B, lower panel). In the 4xbm mimetic structure of full-length Nell-1 and Nell-1-ΔE, three differences were detected between the two isoforms: (1) a beta sheet was present in the p.611-p.621 region of Nell-1 and the p.581-p.591 region of Nell-1-ΔE, but greater differences were observed in the angle between the two beta sheets and the preceding sequence; (2) a small alpha helix occupied the p.658-p.660 region of Nell-1, but a beta sheet was present in the p.653-p.669 region of Nell-1-ΔE; and (3) a smaller alpha helix

FIGURE 1 Predicted domains and structures of full-length Nell-1 and Nell-1-ΔE. A, Prediction of putative domains of full-length Nell-1 and Nell-1-ΔE using SMART, with modifications. Full-length Nell-1 contains one secretory signal peptide, one NH$_2$-terminal thrombospondin-1-like domain (overlapping with a laminin G module), four vWC domains, and six EGF-like domains (the second and fifth are calcium-binding EGF-like domains), whereas Nell-1-ΔE lacks the second calcium-binding EGF-like domain. B, Homology modeling by SWISS-MODEL showed three obvious structural differences between the two isoforms. Green indicates the 5th calcium-binding EGF-like domain present in full-length Nell-1 and absent in Nell-1-ΔE. The red arrows show the three obvious differences observed between full-length Nell-1 and Nell-1-ΔE

was present in the p.679-p.680 region of Nell-1 relative to Nell-1-ΔE, whereas the alpha helix in the p.686-p.690 region of Nell-1-ΔE was larger relative to Nell-1 (Figure 1B, upper panel). We also noted three obvious structural differences in the homology modeling of 4neh: (1) a helical structure was present in the p.477-p.479 region of Nell-1, with no counterpart in Nell-1-ΔE; (2) a beta sheet was present in the p.535-p.572 region of Nell-1, but there was no structure near this sequence; and (3) an alpha helix was present in the p.550-p.552 region of Nell-1, whereas a beta sheet was present in the p.527-p.535 region of Nell-1-ΔE (Figure 1B, lower panel).

3.2 | Nell-1-ΔE, but not full-length nell-1, inhibits cell migration

Full-length Nell-1 and Nell-1-ΔE proteins were overexpressed in HEK-293T cells, and the recombinant forms of these two isoforms were purified. When LoVo cells reached confluence in 6-well plates, scratch wounds were introduced to the monolayers. The cells were then exposed to the full-length Nell-1 or Nell-1-ΔE recombinant protein. After 24 h, cells that had been exposed to Nell-1-ΔE migrated approximately 40% slower than cell that had been exposed to full-length Nell-1 or a
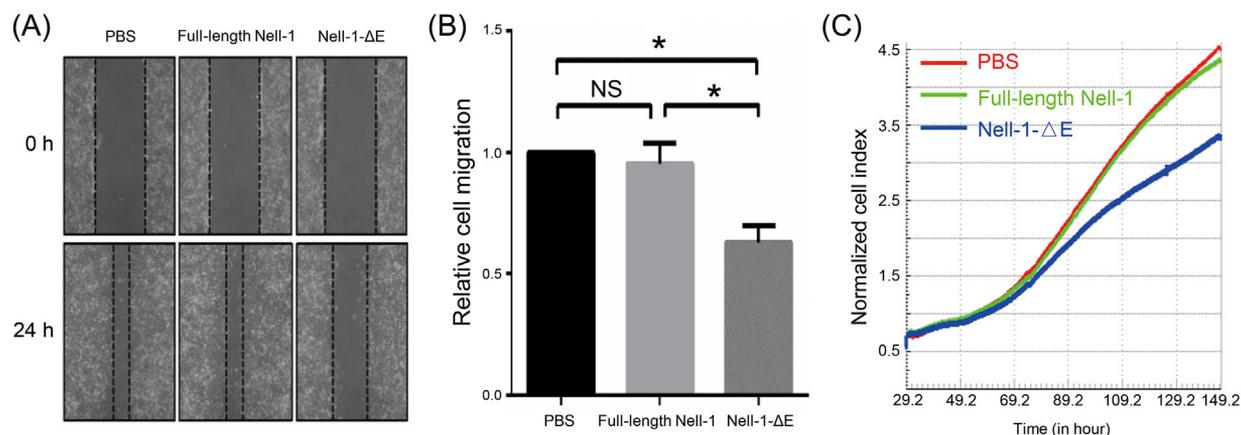
negative control (PBS). However, full-length Nell-1 could not inhibit cell migration (Figures 2A and 2B).

We next seeded LoVo cells in the medium on the iCELLigence Real-Time Analysis system for 24 ~ 30 h and then treated cells with the full-length Nell-1 or Nell-1-ΔE recombinant protein. Compared with the negative control (PBS), full-length Nell-1 did not inhibit cell migration, whereas Nell-1-ΔE did inhibit migration (Figure 2C).

To avoid the effect of proliferation on the results of migration, we performed the CCK-8 assay and found there was no significant difference in proliferation between LoVo cells exposed to full-length Nell-1 and Nell-1-ΔE (Supplemental Figure S2).

3.3 | Full-length nell-1 and nell-1-ΔE proteins exhibit similar subcellular localizations and expression patterns

OCCM-30 cells were co-transfected with Nell-1-CHERRY and Nell-1-ΔE-GFP, and the subcellular locations of both proteins were observed by confocal microscopy. Both full-length Nell-1 and Nell-1-ΔE were

FIGURE 2 Nell-1-ΔE inhibits cell migration, whereas full-length Nell-1 does not. (A, B) The wound healing assay was performed in LoVo cells. Cells were treated with PBS (negative control) or full-length Nell-1 or Nell-1-ΔE recombinant proteins after scratching. Cells treated with Nell-1-ΔE migrated 40% slower than cells treated with full-length Nell-1 or PBS. Full-length Nell-1 did not inhibit cell migration to a greater degree than the control. C, LoVo cells were seeded in the iCELLigence Real-Time Analysis system, and cells treated with the Nell-1-ΔE recombinant protein migrated more slowly than cells treated with full-length Nell-1 or the negative control

expressed at similar intensities in the cytoplasm. Neither protein was detected in the cell membrane or nucleus (Figure 3A). Nell-1-FLAG and Nell-1-ΔE-FLAG plasmids were overexpressed in OCCM-30 and HEK-293FT cells, respectively. Western blotting analysis of cell lysates demonstrated the presence of both full-length Nell-1 and Nell-1-ΔE in two forms: a protein with a molecular weight of ~90 kDa (before N-glycosylation and oligomerization) and a protein with a molecular weight of ~140 kDa (after N-glycosylation under reducing conditions) (Figure 3B). In the medium, only the N-glycosylated (~140 kDa) form was observed (Figure 3C). These data indicated that at the protein level, Nell-1-ΔE and full-length Nell-1 exhibited similar subcellular localizations and expression patterns.

3.4 | Nell-1-ΔE interacts with ENO-1 in the extracellular space

To investigate the underlying mechanism of Nell-1-ΔE, a GFP empty vector, an NELL-1-GFP plasmid, and an NELL-1-ΔE-GFP plasmid were overexpressed in OCCM-30 or HEK-293FT cells. The media was collected from all cells, and co-IP was performed using an anti-GFP antibody and Protein A Magnetic Beads to probe the collected media. By performing an LC-MS/MS analysis of the co-IP products, we observed that ENO-1 interacted with Nell-1-ΔE but not full-length Nell-1 in the extracellular spaces of both cell lines (Figure 4). For detailed LC-MS/MS data, see Supplementary Table S1.
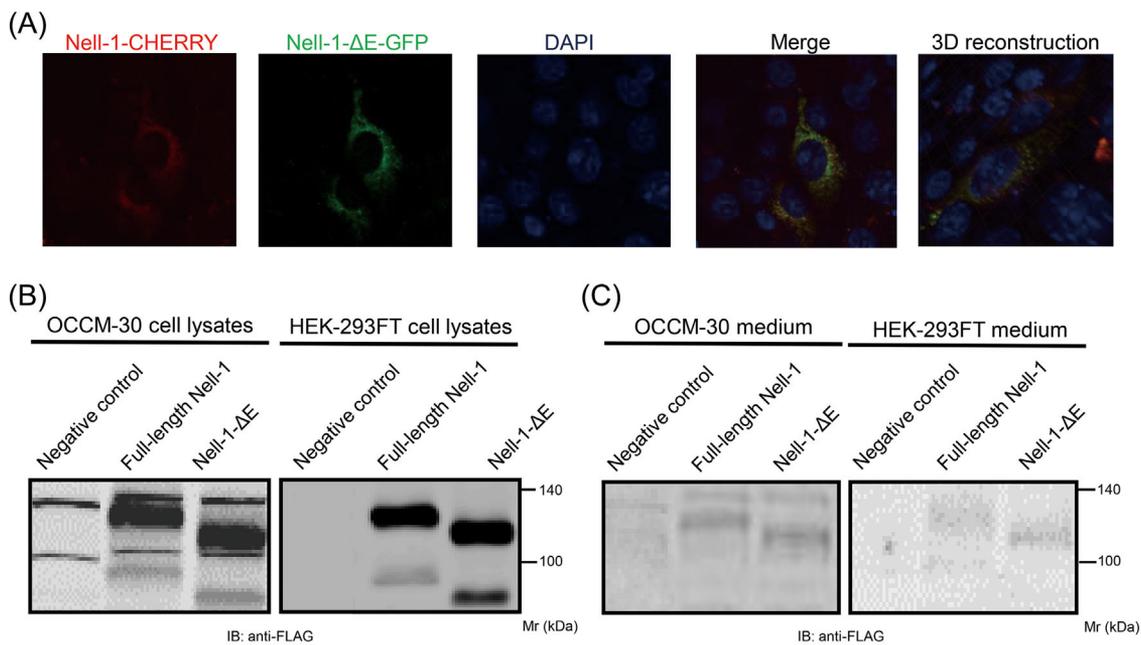
To demonstrate that Nell-1-ΔE inhibits cell migration by interacting with ENO-1, we performed wound healing assay by treating ENO-1-overexpressing LoVo cells with recombinant full-length Nell-1 or Nell-1-ΔE protein. We found that when cells co-treated with ENO-1 and Nell-1-ΔE had a lower rate of migration than cells co-treated with ENO-1 and full-length Nell-1 (Figures 5A and 5B).

4 | DISCUSSION

NELL-1 is a secreted protein that is upregulated in pathologically fusing and fused sutures in patients with non-syndromic unilateral CS.[4] NELL-1 contains one secretory signal peptide, one NH_2-terminal thrombospondin-1-like domain (overlapping with a laminin G module), four vWC domains, and six EGF-like domains (the second and fifth are calcium-binding EGF-like domains).[3] NELL-1 is an osteogenic factor that promotes bone regeneration under many conditions.[12,15–20] A recent study showed that NELL-1 could be used to treat osteoporotic bone loss,[21] and has already been used in a National Aeronautics and Space Administration (NASA) research project to prevent osteoporosis in astronauts (https://www.nasa.gov/).

In our previous study, upon cloning *Nell-1* from a rat cDNA library, a band with a smaller molecular weight than *Nell-1* was detected near the expected band[4] and discovered to be a new transcript of *Nell-1*. Compared with the original *Nell-1* transcript (ie, full-length *Nell-1*), the new transcript lacks a sequence that encodes a calcium-binding EGF-like domain (ie, the fifth EGF-like domain of full-length NELL-1) (Figure 1A). Therefore, this new transcript was named *Nell-1-ΔE*. Considering the important role of calcium-binding EGF-like domains in protein-protein interactions,[8] we speculated that the protein encoded by this novel transcript might have a function and interaction pattern that is distinct from other isoforms.[3,4] By using homology modeling with the structures
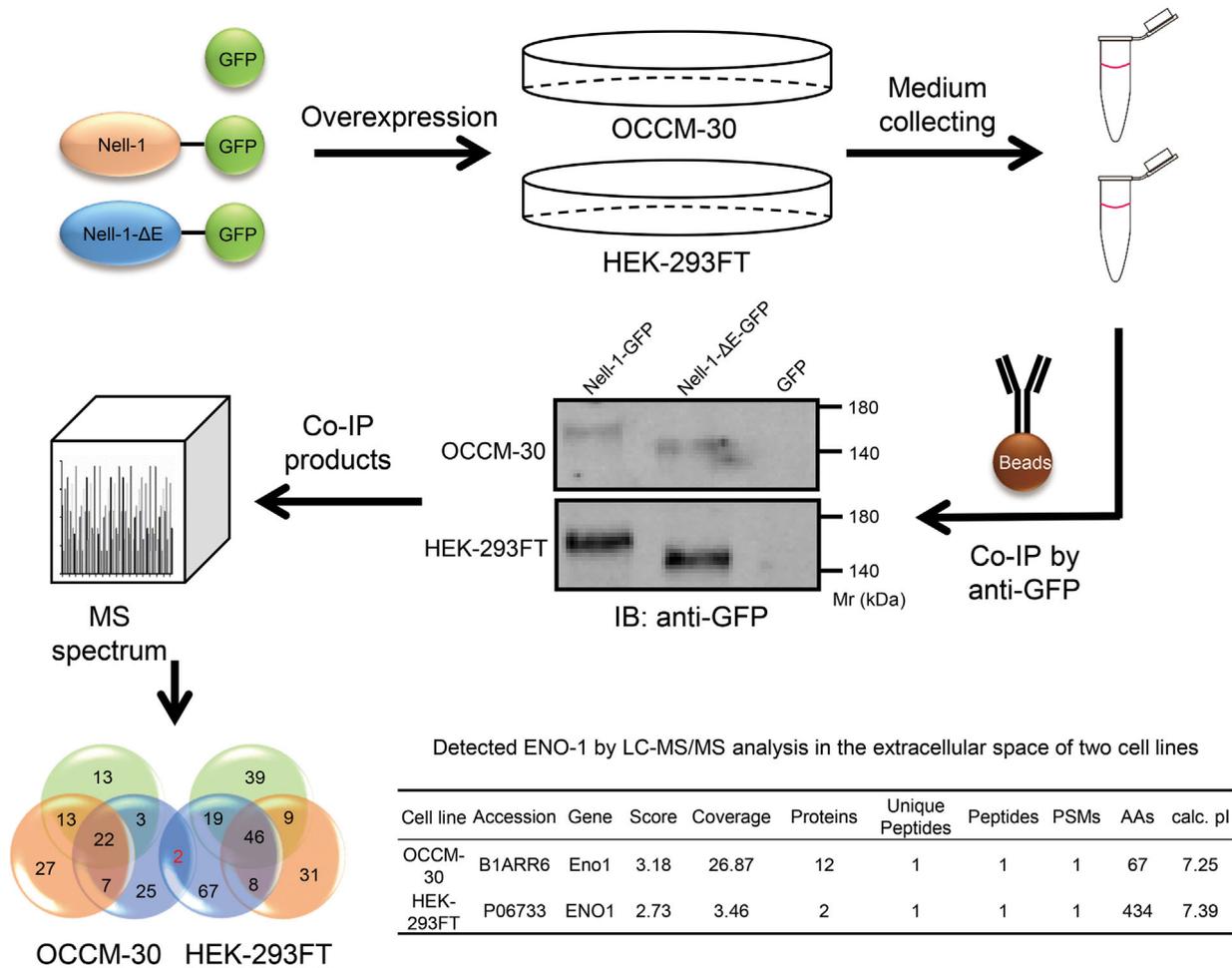
FIGURE 3 The subcellular locations and expression patterns of full-length Nell-1 and Nell-1-ΔE proteins were similar. A, OCCM-30 cells were co-transfected with the Nell-1-CHERRY and Nell-1-ΔE-GFP plasmids. Confocal microscopy showed that both isoforms were localized to the cytoplasm. (B, C) Full-length Nell-1-FLAG and Nell-1-ΔE-FLAG plasmids were overexpressed in OCCM-30 and HEK-293FT cells. The cell lysates and media were analyzed by Western blotting. In the lysates, full-length Nell-1 was present in two forms with the following molecular weights: ~90 kDa (without N-glycosylation) and ~140 kDa (with N-glycosylation). In the extracellular space, only the higher-molecular-weight (ie, the N-glycosylated) form was observed. The expression pattern of Nell-1-ΔE was similar to that of full-length Nell-1

of the two proteins, we discovered obvious structural differences between full-length Nell-1 and Nell-1-ΔE (Figure 1B). This observation further strengthened the hypothesis that Nell-1-ΔE had unique features.

Our initial aim was to compare the endogenous distribution of these two isoforms at the protein level. Antibodies were specifically designed to recognize full-length Nell-1 [including the lacking Ca^{2+}-binding EGF-like domain (YH-CECRSGFHDDGTYSLSGES)] and Nell-1-ΔE [spanning the lacking Ca^{2+}-binding EGF-like domain (GFTGSHCEKDIDE-CALRTHT)]. However, when testing the specificity of these antibodies for the two isoforms, we could not distinguish Nell-1-ΔE from full-length Nell-1 (data not shown). Therefore, we designed primers that spanning the lacking calcium-binding EGF-like domain, which allowing us to distinguish *Nell-1-ΔE* from full-length *Nell-1* by molecular weight (Supplemental Figure S1A). We observed that the ratio of *Nell-1-ΔE*/full-length *Nell-1* was not constant in different regions of the mouse head on E14, E16, and E19 (Supplemental Figure S1B). These results suggest that *Nell-1-ΔE* might have specific functions that are distinct from those of full-length *Nell-1*.

In addition to its role in osteogenesis, NELL-1 is associated with several benign and malignant tumors, including colon cancer,[22] gastric cancer,[23] esophageal adenocarcinoma,[24] and bone tumors.[25] Jin et al[24] found that the NELL-1 promoter was hypermethylated in esophageal adenocarcinoma tissue samples
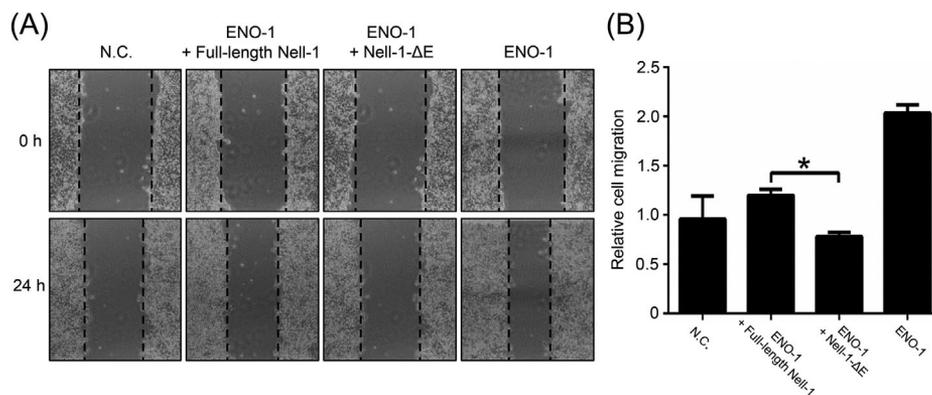
compared with normal esophageal tissue. This phenomenon was also demonstrated in gastric cancer.[23] Shen et al[25] found that NELL-1 exhibited diffuse and reliable expression in benign but not in malignant bone-forming skeletal tumors. These data suggested that *Nell-1* might be a candidate tumor suppressor gene. However, a previous study found that full-length NELL-1 could not inhibit cell proliferation without the assistance of other proteins,[26] which was not consistent with the feature of a candidate tumor suppressor gene. Might there be a similar but not identical transcript of *Nell-1* to play such a role? In the absence of special antibodies against full-length Nell-1 or Nell-1-ΔE, researchers have not been able to determine whether the isoform truly plays a suppressive gene role. Therefore, we used full-length Nell-1 and Nell-1-ΔE recombinant proteins in a cellular wound healing assay and iCELLigence Real-Time Analysis system. We observed that cells treated with Nell-1-ΔE migrated slower than those treated with full-length Nell-1. However, full-length Nell-1 did not inhibit cell migration (Figure 2). This result was quite interesting because it indicated that the Nell-1-ΔE isoform, but not full-length Nell-1, might be important for part of the function of the suppressor gene. Fahmy-Garcia et al[27] found that a high dose of Nell-1 (500 ng/mL) could stimulate MSCs migration and a relatively high dose of Nell-1 (> 100 ng/mL) could stimulate endothelial cell migration. The results were not consistent with our results, as we showed that full-length Nell-1 did not influence migration in LoVo cells and

FIGURE 4 Co-IP and LC-MS/MS shows that only Nell-1-ΔE interacts with ENO-1 in the extracellular spaces of two cell lines. OCCM-30 and HEK-293FT cells were transfected with a GFP empty vector, a full-length Nell-1-GFP plasmid, or a Nell-1-ΔE-GFP plasmid. The cell medium was collected and subjected to co-IP, followed by LC-MS/MS, which identified ENO-1 in the samples from both cell lines that had been in complex with Nell-1-ΔE

that Nell-1-ΔE inhibited migration (Figure 2). Different cells might respond differently in terms of migration in response to a particular stimulus.[28] The differences between cell lines used by Fahmy-Garcia et al and by us might be the main reason behind the discrepancies in migration. Meanwhile, in Fahmy-Garcia et al's study, when the cells were treated with a low dose of Nell-1 protein (< 100 ng/mL), their migratory ability did not change in comparison with the migratory ability of control cells for both

FIGURE 5 ENO-1-overexpressing LoVo cells treated with Nell-1-ΔE had a lower rate of migration than cells treated with full-length Nell-1

MSCs and endothelial cells. These findings were consisting with our results, which treatment with full-length Nell-1 did not result in a significant difference in migration between the control group and the full-length Nell-1-treated group. Moreover, in another study focusing on the effect of Nell-1 on cell migration, researchers found that Nell-1 could inhibit migration in two cancer cell lines (OS-RC-2 and VMRC-RCW).[29]

Furthermore, we observed that the subcellular locations of full-length Nell-1 and Nell-1-ΔE were similar (Figure 3A). We also analyzed the protein expression patterns of full-length Nell-1 and Nell-1-ΔE and found that full-length Nell-1 and Nell-1-ΔE exhibited similar expression patterns at the protein level in both the cell lysates and extracellular space (Figures 3B and 3C), which was consistent with our previous report.[3]

Because Nell-1 is a secreted protein,[1] we pursued the protein(s) that interacted with Nell-1-ΔE in the extracellular space. We overexpressed full-length Nell-1 and Nell-1-ΔE in OCCM-30 or HEK-293FT cells. Using medium collected from the cells, we performed co-IP and further LC-MS/MS analyses. ENO-1 was identified in the samples from both cell lines in which only Nell-1-ΔE was expressed (Figure 4), indicating that Nell-1-ΔE interacted with ENO-1 in the extracellular spaces of both cell lines, which differed from full-length Nell-1.

ENO-1 is primarily thought to be a key enzyme that is involved in the 2-phospho-D-glycerate hydrolase reaction.[30] ENO-1 is reportedly overexpressed in several types of human cancer[31] and plays an important role in the formation of benign or malignant tumors.[32] ENO-1 can exteriorize to the extracellular space via STIM1/ORAI1-mediated Ca^{2+} influx[33] and promote cell migration[34,35] by acting as an oncogene. Negative regulation of the ENO-1 function by the FBXW7 protein has been observed through its interaction with ENO-1. Researchers have speculated that ENO-1 might be blocked by FBXW7 when ENO-1 interacting with FBXW7, with consequent FBXW7-mediated suppression of the ENO-1 function.[36] A similar observation was made regarding the interaction between protease 2A and ENO-1, in which protease 2A blocked ENO-1 and prevented the normal function of ENO-1 during the protease 2A/ENO-1 interaction.[37]

In this study, we observed an interaction between Nell-1-ΔE and ENO-1 in the extracellular spaces of two cell lines (Figure 4). Based on our existing data, we came up with the following hypothesis: Nell-1-ΔE but not full-length Nell-1 can interact with extracellular ENO-1, a cell migration-promoting factor, and blocks the functional domain of ENO-1, thereby negatively affecting the oncogenic function of ENO-1, consequently inhibiting cell migration. In this regard, Nell-1-ΔE exhibited a characteristic of a suppressor gene. To verify that this interaction exists in LoVo cells and to prove the hypothesis that Nell-1-ΔE inhibits cell migration by interacting with ENO-1, we conducted wound healing assay by treating ENO-1-overexpressing LoVo cells with full-length Nell-1 or Nell-1-ΔE recombinant proteins (Figure 5). ENO-1-overexpressing LoVo cells migrate at a higher rate than parental LoVo cells, consistent with oncogenic

characteristics of ENO-1.[34,35] However, ENO-1-overexpressing LoVo cells treated with Nell-1-ΔE had a lower rate of migration than did the cells treated with full-length Nell-1, indicating that the extracellular ENO-1 might be blocked because of its interaction with Nell-1-ΔE but not full-length Nell-1. However, because the evidence for the interaction between Nell-1-ΔE and ENO-1 is preliminary, further investigation and more evidences including data from a phage display library[26] are warranted to confirm this phenomenon in future studies. Additionally, the nature of the biochemical interaction between Nell-1-ΔE and ENO-1 should be clarified to develop a further understanding of the function and mechanism of Nell-1-ΔE.

In summary, we identified a novel transcript of *Nell-1*. Due to the absence of a sequence encoding a calcium-binding EGF-like domain compared with full-length *Nell-1*, we named the transcript *Nell-1-ΔE*. Nell-1-ΔE exhibited properties that were similar but not identical to those of full-length Nell-1, especially regarding inhibition of cell migration. Using co-IP and LC-MS/MS, we demonstrated that Nell-1-ΔE interacts with ENO-1 in the extracellular space.

ACKNOWLEDGEMENTS

CONFLICTS OF INTEREST

Drs. X.Z. and K.T. are inventors of Nell-1 related patents. Drs. X.Z. and K.T. are founders of Bone Biologics Inc./Bone Biologics Corp. which sublicenses Nell-1 patents from the UC Regents, which also hold equity in the company.

ORCID

Huaxiang Zhao http://orcid.org/0000-0002-9661-0166

REFERENCES

1. Kuroda S, Oyasu M, Kawakami M, et al. Biochemical characterization and expression analysis of neural thrombospondin-1-like proteins NELL1 and NELL2. *Biochem Biophys Res Commun*. 1999;265:79–86.
2. Watanabe TK, Katagiri T, Suzuki M, et al. Cloning and characterization of two novel human cdnas (NELL1 and NELL2) encoding proteins with six EGF-like repeats. *Genomics*. 1996;38:273–276.
3. Zhang X, Zara J, Siu RK, Ting K, Soo C. The role of NELL-1, a growth factor associated with craniosynostosis, in promoting bone regeneration. *J Dent Res*. 2010;89:865–878.
4. Ting K, Vastardis H, Mulliken JB, et al. Human NELL-1 expressed in unilateral coronal synostosis. *J Bone Miner Res*. 1999;14:80–89.

5. Desai J, Shannon ME, Johnson MD, et al. Nell1-deficient mice have reduced expression of extracellular matrix proteins causing cranial and vertebral defects. *Hum Mol Genet*. 2006;15:1329–1341.

6. Zhang X, Kuroda S, Carpenter D, et al. Craniosynostosis in transgenic mice overexpressing Nell-1. *J Clin Invest*. 2002;110:861–870.

7. Pang S, Shen J, Liu Y, et al. Proliferation and osteogenic differentiation of mesenchymal stem cells induced by a short isoform of NELL-1. *Stem Cells*. 2015;33:904–915.

8. Rao Z, Handford P, Mayhew M, Knott V, Brownlee GG, Stuart D. The structure of a Ca²⁺-binding epidermal growth factor-like domain: its role in protein-protein interactions. *Cell*. 1995;82:131–141.

9. Kim HS, Lee DS, Lee JH, et al. The effect of odontoblast conditioned media and dentin non-collagenous proteins on the differentiation and mineralization of cementoblasts in vitro. *Arch Oral Biol*. 2009;54:71–79.

10. Zhang YY, Zhao HX, Chen ZB, Lin JX, Liu Y. Osteoprotegerin promotes cementoblastic activity of murine cementoblast cell line in vitro. *Chin J Dent Res*. 2016;19:103–108.

11. Yan X, Liao H, Cheng M, et al. Smad7 protein interacts with receptor-regulated smads (R-Smads) to inhibit transforming growth factor-beta (TGF-beta)/Smad signaling. *J Biol Chem*. 2016;291:382–392.

12. Zhang X, Ting K, Bessette CM, et al. Nell-1, a key functional mediator of Runx2, partially rescues calvarial defects in Runx2 (+/−) mice. *J Bone Miner Res*. 2011;26:777–791.

13. Aras B, Yerlikaya A. Bortezomib and etoposide combinations exert synergistic effects on the human prostate cancer cell line PC-3. *Oncol Lett*. 2016;11:3179–3184.

14. Wang Q, Zhou JL, Wang H, et al. Inhibition effect of cypermethrin mediated by co-regulators SRC-1 and SMRT in interleukin-6-induced androgen receptor activation. *Chemosphere*. 2016;158:24–29.

15. Aghaloo T, Cowan CM, Chou Y-F, et al. Nell-1-induced bone regeneration in calvarial defects. *Am J Pathol*. 2006;169:903–915.

16. Cowan CM, Cheng S, Ting K, et al. Nell-1 induced bone formation within the distracted intermaxillary suture. *Bone*. 2006;38:48–58.

17. Aghaloo T, Cowan CM, Zhang X, et al. The effect of NELL1 and bone morphogenetic protein-2 on calvarial bone regeneration. *J Oral Maxillofac Surg*. 2010;68:300–308.

18. Lu SS, Zhang X, Soo C, et al. The osteoinductive properties of Nell-1 in a rat spinal fusion model. *Spine J*. 2007;7:50–60.

19. James AW, Pan A, Chiang M, et al. A new function of Nell-1 protein in repressing adipogenic differentiation. *Biochem Biophys Res Commun*. 2011;411:126–131.

20. James AW, Pang S, Askarinam A, et al. Additive effects of sonic hedgehog and Nell-1 signaling in osteogenic versus adipogenic differentiation of human adipose-derived stromal cells. *Stem Cells Dev*. 2012;21:2170–2178.

21. James AW, Shen J, Zhang X, et al. NELL-1 in the treatment of osteoporotic bone loss. *Nat Commun*. 2015;6:7362.

22. Mori Y, Cai K, Cheng Y, et al. A genome-wide search identifies epigenetic silencing of somatostatin, tachykinin-1, and 5 other genes in colon cancer. *Gastroenterology*. 2006;131:797–808.

23. Gao C, Zhang Q, Kong D, et al. Maldi-tof mass array analysis of *Nell-1* promoter methylation patterns in human gastric cancer. *Biomed Res Int*. 2015;2015:136941.

24. Jin Z, Mori Y, Yang J, et al. Hypermethylation of the nel-like 1 gene is a common and early event and is associated with poor prognosis in early-stage esophageal adenocarcinoma. *Oncogene*. 2007;26:6332–6340.

25. Shen J, LaChaud G, Khadarian K, et al. NELL-1 expression in benign and malignant bone tumors. *Biochem Biophys Res Commun*. 2015;460:368–374.

26. Zou X, Shen J, Chen F, et al. NELL-1 binds to APR3 affecting human osteoblast proliferation and differentiation. *FEBS Lett*. 2011;585:2410–2418.

27. Fahmy-Garcia S, van Driel M, Witte-Buoma J, et al. Nell-1, HMGB1 and CCN2 enhance migration and vasculogenesis, but not osteogenic differentiation compared to BMP2. *Tissue Eng Part A*. 2018;24:207–218.

28. Kang SU, Kim YS, Kim YE, et al. Opposite effects of non-thermal plasma on cell migration and collagen production in keloid and normal fibroblasts. *PLoS ONE*. 2017;12:e0187978.

29. Nakamura R, Oyama T, Tajiri R, et al. Expression and regulatory effects on cancer cell behavior of NELL1 and NELL2 in human renal cell carcinoma. *Cancer Sci*. 2015;106:656–664.

30. Poyner RR, Reed GH. Structure of the bis divalent cation complex with phosphonoacetohydroxamate at the active site of enolase. *Biochemistry*. 1992;31:7166–7173.

31. Capello M, Ferri-Borgogno S, Cappello P, Novelli F. Alpha-enolase: a promising therapeutic and diagnostic tumor target. *FEBS J*. 2011;278:1064–1074.

32. Altenberg B, Greulich KO. Genes of glycolysis are ubiquitously overexpressed in 24 cancer classes. *Genomics*. 2004;84:1014–1020.

33. Didiasova M, Zakrzewicz D, Magdolen V, et al. STIM1/ORAI1-mediated Ca²⁺ influx regulates enolase-1 exteriorization. *J Biol Chem*. 2015;290:11983–11999.

34. Yu L, Shi J, Cheng S, et al. Estrogen promotes prostate cancer cell migration via paracrine release of ENO1 from stromal cells. *Mol Endocrinol*. 2012;26:1521–1530.

35. Zakrzewicz D, Didiasova M, Zakrzewicz A, et al. The interaction of enolase-1 with caveolae-associated proteins regulates its subcellular localization. *Biochem J*. 2014;460:295–307.

36. Zhan P, Wang Y, Zhao S, et al. Fbxw7 negatively regulates ENO1 expression and function in colorectal cancer. *Lab Invest*. 2015;95:995–1004.

37. Zhao T, Huang X, Xia Y. Human heart cell proteins interacting with a C-terminally truncated 2A protein of coxsackie B3 virus: identification by the yeast two-hybrid system. *Virus Genes*. 2016;52:172–178.

SUPPORTING INFORMATION

Additional Supporting Information may be found online in the supporting information tab for this article.